Bone 49 (2011) 931–938

Contents lists available at ScienceDirect

Bone

journal homepage: www.elsevier.com/locate/bone

Original Full Length Article

Deriving tissue density and elastic modulus from microCT bone scans☆

David W. Wagner *, Derek P. Lindsey, Gary S. Beaupre

VA Palo Alto Health Care System, Bone and Joint Center, USA

ARTICLE INFO

Article history:
Received 18 April 2011
Revised 13 July 2011
Accepted 14 July 2011
Available online 23 July 2011

Edited by: David Fyhrie

Keywords:
Bone mineralization
Tissue density
Elastic modulus
Mineral density
Micro-computed tomography

ABSTRACT

Tissue level density and elastic modulus are intrinsic properties that can be used to quantify bone material and analyses incorporating those quantities have been used to evaluate bone on a macroscopic scale. Micro-computed tomography (microCT) technology has been used to construct tissue level finite element models to simulate macroscopic fracture strength, however, a single method for assigning voxel-specific tissue density and elastic modulus based on those data has not been universally accepted. One method prevalent in the literature utilizes an empirical relationship that derives tissue stiffness as a function of bone calcium content weight fraction. To derive calcium content weight fraction from microCT scans, a measure of tissue density is required and a constant value is traditionally used. However, experimental data suggest a non-trivial amount of tissue heterogeneity suggesting a constant tissue density may not be appropriate. A theoretical derivation for determining the relationship between voxel-specific tissue density and microCT scan data (i.e., microCT derived tissue mineral density (TMD), mgHA/cm^3) and bone constituent properties is proposed. Constant model parameters used in the derivation include the density of water, ash, and organics (i.e., bone constituents) and the volume fraction of the organics constituent. The effect of incorporating the theoretically derived tissue density (instead of a constant value) in determining voxel-specific elastic modulus resulted in a maximum observed increase of 12 GPa (5.9 GPa versus 17.9 GPa, for the constant value and derived tissue density formulations, respectively) for a measured TMD of 1.02 gHA/cm^3. Average and bounding quantities for the four constant model parameters were defined from the literature and the influence of those values on the derived tissue density and elastic modulus relationships were also evaluated. The theoretical relationships of tissue density and elastic modulus, with the average constant model parameters applied, were consistent with previously published empirical relationships derived from experimental data. Tissue density as a function of microCT TMD was formulated as a linear relationship and the density of water and ash was shown to solely influence the proportionality (i.e., slope) between those values. The density of water and organics (i.e., collagen) and the volume fraction of the organics constituent were shown to influence the constant offset (intercept) between tissue density and TMD with no influence from ash density. Incorporating tissue density heterogeneity into the derivation of elastic modulus resulted in a significant increase in predicted modulus (for microCT TMD ranges observed for healthy tissue) as compared to when a constant tissue density was used. The presented approach provides a novel method for deriving tissue-level bone material properties and quantifies the effect of assuming tissue homogeneity when calculating elastic modulus (when using a prevalent method in the literature) from microCT scan data.

Published by Elsevier Inc.

Introduction

Micro-computed tomography (microCT) has become a popular method for quantifying and analyzing bone structure [1–4] and degree of bone mineralization [5,6]. Although well suited for quantifying bone structure, CT-based technology is limited to only providing information related to bone mineral content. This limitation is best exemplified in how bone density is traditionally reported, as an equivalent tissue mineral density (TMD), usually defined in relation to a calibration phantom of similar material (e.g., mg-Hydroxyapaptite per cm^3). A common implementation of this technique defines a linear relationship between microCT-derived linear attenuation and known hydroxyapatite contents from a calibration phantom [1,3,6,7]. Hydroxyapatite equivalent tissue mineral density is then assigned during in-vivo scans on a voxel-by-voxel basis using the attenuation to hydroxyapatite content relationship derived for that particular CT scanner. The true tissue density of the scanned bone tissue is traditionally not calculated nor reported.

Tissue density is an intrinsic material property and quantifying that value using an in-vivo CT scan would help integrate previous density-derived experimental relationships with image-based analysis measures

☆ Conflict of interest: All authors state that they have no conflicts of interest.

* Corresponding author at: VA Palo Alto Health Care System, Bone and Joint Center, 3801 Miranda Avenue, Building 51, Mail Stop 153, Palo Alto, CA, USA. Fax: +1 650 849 0580.

E-mail addresses: dwwagner@va51.stanford.edu (D.W. Wagner), lindsey@va51.stanford.edu (D.P. Lindsey), beaupre@va51.stanford.edu (G.S. Beaupre).

8756-3282/$ – see front matter. Published by Elsevier Inc.
doi:10.1016/j.bone.2011.07.021

using consistent metrics. Although tissue mineral density has been used to quantify changes in bone tissue as related to a variety of factors [5,6,8–11], TMD represents only one constituent of bone (i.e., the mineral phase) and ignores the contributions of the organic and water phases. This omission leads to a discrepancy in the numerical scales when comparing tissue mineral density and other defined densities (e.g., apparent density, which is hypothetically equivalent to ~~TMD~~ for dense cortical bone [12]) making direct comparisons between image CT derived density and gravimetric derived densities extremely difficult. Only recently has the relationship between TMD and apparent density begun to be examined experimentally [12]. To confuse the issue further, it is possible to calculate a microCT apparent density based on the tissue mineral density by incorporating segmented structures (e.g., Scanco (IPL v1.12, Scanco Medical AG) reports this metric as "Mean1" in units of mgHA/cm^3). However this microCT apparent density suffers from the same limitation as previously described and cannot be directly compared to gravimetrically derived apparent densities even though they share the same name. A method for calculating tissue density directly from microCT TMD would bridge this gap and allow for apparent densities derived from microCT scans to be in the same units and directly comparable to gravimetrically determined apparent densities.

A natural extension of the microCT technology has been the application of micro-finite element models, in which element sizes are less than 100 μm, as predictive tools for estimating bone stiffness and strength [13,14]. These 'tissue-level' models, named because the tissue structure of the trabecular bone can be modeled, have been used to evaluate the contribution of trabecular structure and properties to overall bone strength. The application of these microFE models have traditionally been performed with homogenous material properties [13,15], however several articles have suggested the importance of incorporating material heterogeneity [11,16–18]. Several methods have been proposed for including heterogeneity in the material property assignment of tissue level models [7,11,16,18]. Unfortunately, a single protocol for assigning an isotropic elastic modulus on a voxel by voxel basis has not been universally accepted, although several are prevalent.

One particular method that has been used in several recent papers [6,18–21] assigns the elastic modulus of individual voxel elements based on the linear attenuation for that voxel. Such a method addresses an important need of how to appropriately assign material heterogeneity from microCT derived hydroxyapatite (HA) density. One crucial step involved in this method is that the microCT derived HA density is converted into a mass fraction by assuming a constant tissue density of the underlying bone (potentially in part because no viable method was available for deriving tissue density from the microCT scan). However, using gravimetric methods, Day [22] reported a range of tissue densities from 35 donors (age 38 to 85 years) for dried, defatted specimens taken from 15 samples from each cadaveric proximal tibiae, with the specimen averages ranging from 2.11 to 2.33 g/cm^3 and an average standard deviation across the donors of 0.036 g/cm^3. Hernandez et al. [23] found tissue densities ranging from 1.634 to 2.26 g/cm^3 for vertebral and femoral bone samples. The actual range of tissue densities observed on a voxel by voxel basis with microCT is potentially much larger, as the reported values above are derived from mature bone, and will not accurately represent unmineralized tissue (i.e., osteoid) or bone in the early phases of mineralization. This observation is supported by the large range (varying by over a factor of 3) of reported synchrotron and microCT derived HA densities of bone [3] within a single specimen. Using contact microradiography, Boivin and Meunier [24] measured the degree of bone mineralization from iliac bone samples and showed ranges of measurements varying by a factor of 2. Wagner and Beaupre [25] found that the ratio of hydroxyapatite (HA) density to tissue density is critical to the derived magnitude of elastic modulus in the procedure described above, raising a concern as to the validity of assuming a constant tissue density as well as the appropriateness of the selected constant value.

A theoretical method for determining voxel-specific tissue density derived from microCT scan data has yet to be defined. The purpose of the present study is to propose such a method based on the known constituents of bone, evaluate the assumptions inherent to the method, and quantify the robustness of the predicted tissue-density and elastic modulus to perturbations of parameters assumed during the model derivation.

Methods

Voxel-based tissue density derivation

The primary output from a microCT scan is a voxel-based gray scale or attenuation value that is typically converted to an equivalent hydroxyapatite density, based on the use of a manufacturer-specific calibration curve. The true bone tissue density, however, is not directly measured during a microCT scan. Although an equivalent HA density is calculated for each voxel, it should be made clear that this value is not equivalent to the true tissue density (i.e., mass of bone material/volume of bone material), but is the density of a material with an equivalent mineral content as the scanned voxel [26]. This value may be more appropriately named the "equivalent mineral" density, or as referred to in some microCT-based studies [9,10,27], tissue mineral density (TMD). A method for deriving the true tissue density (on a voxel scale level) from microCT scan derived equivalent density is proposed followed by incorporating those results to yield a derived elastic modulus. The calculation of true tissue density from mineral density begins with the following assumptions and definitions regarding the constituents of bone.

Assumption 1. The underlying constituents of bone at the microCT voxel level are water, organics, and ash.

We define V_x to be the volume of a constituent (x = w (water), o (organics), a (ash)) or the tissue (x = t). We define m_x to be the mass of a constituent (x = w, o, a) or the tissue (x = t).

Based on the bone composition, the following equations can be defined:

$$V_t = V_w + V_o + V_a, \tag{1a}$$

and

$$m_t = m_w + m_o + m_a. \tag{1b}$$

Martin [28] reported a similar equation to Eq. (1a) that included an additional constituent term of V_v, representing the void volume contribution to the overall tissue volume. Martin [28] used V_v in the context of bone porosity, probably in relation to bone specimens on a scale larger than 100 μm. However in the context of microCT with a voxel of thresholded bone with a scale on the order of 10 to 100 μm, we assume here that the contribution of void volume is negligible and that the 'V_v' term can be excluded from the derivation. Our analysis also does not consider surface voxels with potential partial volume errors. Typically such voxels are removed by a "peeling" procedure prior to performing any microCT analyses that are sensitive to partial volume errors [29,30].

Based on the previous definitions, the following relationship can be defined:

$$m_x = \rho_x \cdot V_x, \tag{2}$$

where ρ_x represents the density of each constituent. Tissue density (ρ_t) will be calculated as:

$$\rho_t = m_t / V_t = (m_w + m_o + m_a) / V_t, \tag{3}$$

where V_t is the tissue volume and is defined here as the microCT scan voxel volume. The next sections derive equations for each of the constituent masses, m_a, m_o, and m_w.

The mass of the ash constituent (m_a) in the voxel volume, V_t, is calculated from the microCT equivalent HA density (ρ_{HA}) for the same voxel [31]. From Eq. (2) and knowledge that ρ_{HA} is the mineral density of an equivalent material (i.e., calibration HA phantom),

$$m_a = \rho_{HA} \cdot V_t. \quad (4)$$

Calculation of the organics mass component (m_o) requires the following assumption.

Assumption 2. The volume fraction (R_o) of the organics constituent of bone is constant.

The volume of the organics component can be calculated as:

$$V_o = R_o \cdot V_t. \quad (5)$$

Therefore, the mass of the organics component can be calculated as:

$$m_o = \rho_o \cdot V_o = \rho_o \cdot R_o \cdot V_t. \quad (6)$$

The mass of the water constituent (m_w) is calculated by first identifying a significant implication related to Assumption 2. That is, if V_o is constant and Eq. (1a) defines the relationship between the constant total volume of the scanned voxel and the underlying constituents, then the sum of V_a and V_w must also be constant. This relationship can be restated as changes in the volume of the ash constituent (V_a) are compensated by equivalent changes in the volume of the water constituent (V_w), and vice versa [28,32,33].

Combining Eqs. (1a) and (5) yields the following relationship:

$$V_w = (1-R_o) \cdot V_t - V_a. \quad (7)$$

Combining Eqs. (2) and (7) results in:

$$m_w = \rho_w \cdot ((1-R_o) \cdot V_t - V_a).$$

Substituting V_a for the relationship defined when Eqs. (4) and (2) are combined yields:

$$m_w = \rho_w \cdot ((1-R_o) \cdot V_t - (\rho_{HA} \cdot V_t) / \rho_a). \quad (8)$$

The relationships for m_w, m_o, and m_a can be used with Eq. (3) to define the following tissue density relationship:

$$\rho_t = (m_w + m_o + m_a) / V_t,$$
$$\rho_t = (\rho_w \cdot ((1-R_o) \cdot V_t - (\rho_{HA} \cdot V_t) / \rho_a) + (\rho_o \cdot R_o \cdot V_t) + (\rho_{HA} \cdot V_t)) / V_t.$$

Simplifying this equation and grouping the terms to be consistent with the formula of a straight line ($y = mx + b$), where ρ_t is 'y' and ρ_{HA} is 'x', yield:

$$\rho_t = [1-(\rho_w / \rho_a)] \cdot \rho_{HA} + [R_o \cdot (\rho_o - \rho_w) + \rho_w]. \quad (9)$$

Voxel-based elastic modulus derivation

The relationship for the tissue density defined by Eq. (9) can be incorporated into the procedure presented by Renders et al. [18] to compute the elastic modulus from the microCT mineral density. One step in the procedure presented by Renders et al. [18] is the calculation of the calcium content within the microCT voxel, which is given as:

$$[Ca] = (0.4 \cdot \rho_{HA} \cdot 1000 / \rho_t) \cdot B, \quad (10)$$

where [Ca] is the calcium content in mg Calcium/g-dry defatted bone within the microCT voxel. The quantity, 0.4, is the fraction of calcium in hydroxyapatite [34]. The number 1000 is a factor to convert ρ_{HA} from units gHA/cm^3 into the units of mgHA/cm^3. The parameter, *B*, is a conversion factor to convert the calcium content from the units of mg Ca/g-wet defatted bone to mg Ca/g-dry defatted bone and acts on the value of ρ_t in the denominator of the calcium content weight ratio. In the context of microCT, *B* is a factor that scales the weight of wet bone to the weight of dry bone in a scanned voxel. O'Flaherty [35] reported an average value of 1.208 as the weight fraction of wet bone to dry bone, however *B* can also be defined using the bone constituents as:

$$B = \text{wet weight} / \text{dry weight} = (m_a + m_o + m_w) / (m_a + m_o).$$

Incorporating the relationships previously defined for the individual constituent masses,

$$B = (\rho_{HA} \cdot (1-(\rho_w / \rho_a)) + R_o \cdot (\rho_o - \rho_w) + \rho_w) / (\rho_{HA} + \rho_o \cdot R_o). \quad (11)$$

It should be noted that *B* is a function of ρ_{HA} and is therefore not constant, as implied by the single average value reported by O'Flaherty [35]. The equation from Currey [36] relating calcium content, [Ca], to elastic modulus is:

$$\log_{10}(E_t) = -8.58 + 4.05 \cdot \log_{10}[Ca]. \quad (12)$$

Combining Eqs. (9), (10), (11), and (12) and simplifying the result yield the direct relationship between voxel-level elastic modulus, microCT-derived HA density, bone constituent densities, and the organics volume fraction:

$$\log_{10}(E_t) = -8.58 + 4.05 \cdot \log_{10}(400 \cdot \rho_{HA} / (\rho_{HA} + \rho_o \cdot R_o)). \quad (13)$$

Defining average and bounds to the baseline model parameters

Martin [28] suggested constituent and organics volume fraction values (used later as baseline model parameters) of:

$$R_o = 0.36,$$
$$\rho_w = 1.0\ g/cm^3,$$
$$\rho_o = 1.4\ g/cm^3,$$
$$\rho_a = 3.0\ g/cm^3.$$

Using those values for ρ_o and R_o, Eq. (13) becomes:

$$\log_{10}(E_t) = -8.58 + 4.05 \cdot \log_{10}(400 / (1 + (0.504 / \rho_{HA}))), \quad (14)$$

where ρ_{HA} is in gHA/cm^3 and E_t is in GPa. Eqs. (13) and (14) apply to wet bone.

The derived relationship between microCT and tissue density utilizes four parameters: the density of the three bone constituents (water, ash, and organics) and the volume fraction of the organics constituent. The density of water is known (1.0 g/cm^3) and the effects related to perturbations to this value are not discussed.

The selection of the constant ratio representing the percent organic constituent volume (R_o) is critical to the derivation above and the presented results. From Eq. (9), the percent organic constituent volume (R_o) can be seen to be proportional to the intercept of the defined linear relationship between the mineral and tissue density, although it should be noted that the direct effect of R_o is confounded by the magnitude of the difference between the density of the organics constituent and the density of water. Elliott and Robinson [37] suggested a value of 32% for the volume of the organic constituent of whole dog bones. Gong et al. [38] reported similar average organic volume fractions for cortical and trabecular bone specimens of four different species (Table 1). Robinson [32] reported values of 35.56% and 38.18% for dog bone samples classified with two different "osteoid" patterns. A nominal value of 36% [28] was selected as a baseline value. Based on the ranges and standard

Table 1
Summary of organic constituent volume fraction reported in the literature, grouped by species and ordered by magnitude.

Study	Percent organic constituent volume ($R_o \pm$ std dev.)[a]	Species	Bone type
Elliott and Robinson [37]	32	Dog	Whole bone (find this out)
Gong et al. [38][a]	34.5 ± 0.011	Dog	Trabecular
Robinson [32]	35.56	Dog	Tibial cortex, osteoid pattern 'B'
Gong et al. [38]	36.3 ± 0.006	Dog	Cortical
Robinson [32]	38.18	Dog	Tibial cortex, osteoid pattern 'A'
Gong et al. [38]	33.8 ± 0.005	Human	Cortical
Gong et al. [38]	34.9 ± 0.005	Human	Trabecular
Gong et al. [38]	33.7 ± 0.011	Monkey	Cortical
Gong et al. [38]	36.1 ± 0.013	Monkey	Trabecular
Gong et al. [38]	33.6 ± 0.008	Steer	Cortical
Gong et al. [38]	34.2 ± 0.006	Steer	Trabecular

[a] Standard deviations were only available for Gong et al. [38]. Each standard deviation was calculated using the same method described by Gong et al. [38] for deriving the percent organic volume averages by dividing the reported measured weight per volume of the organics by an assumed organic density of 1.426 g/cm^3.

deviations in Table 1, a conservative estimate on the range of plausible values for the organic constituent volume was selected to be from 30% to 40% (used in the subsequent analysis).

The value of the ash constituent density (ρ_a) is proportionally related to the slope of the relationship between mineral and tissue density (Eq. (9)). Currey [39] suggested a value of 3.2 g/cm^3 for the ash density and Gong et al. [40] used a value of 3.18. Robinson [32] identified a range of bone apatite densities between 2.85 and 3.15 g/cm^3. The effects of two different ash densities of 3.2 and 2.85 g/cm^3 are compared with the baseline model value of 3.0 g/cm^3 on the derivations above.

The value of the organics constituent density (ρ_o), similar to the organics constituent volume fraction, affects the intercept of the linear relationship between the mineral and tissue density. Currey [39] suggested a value of 1.1 g/cm^3 for the density of the organic constituents while Bear [41], Elliott and Robinson [37], and Gong et al. [40] reported values of 1.41, 1.45, and 1.426 g/cm^3, respectively. The effects of two different organics density of 1.1 and 1.45 g/cm^3 are compared with the baseline model value of 1.4 g/cm^3 on the derivations above.

Results

Mineral density versus tissue density and elastic modulus relationships with the baseline model parameters

Tissue density as a function of microCT density is plotted in Fig. 1 for the baseline parameter values defined in the previous derivation. The microCT density values in Fig. 1 are plotted over the range of 0 to 1.920 gHA/cm^3, defined by the physical limits (i.e., mass of mineral ≥0 and mass of water ≥0) implicit in Eq. (9) and the selected baseline model parameters. For the microCT densities of 0.4 and 1.2 gHA/cm^3 (HA densities in microCT bone scans are often found in this range), the corresponding tissue density values are 1.41 and 1.94 g/cm^3, respectively.

Elastic moduli derived from microCT density and the baseline model parameters previously listed (Eq. (14)) are plotted in Fig. 2. The effect of utilizing a constant tissue density in Eq. (10) ($\rho_t = 2.0$ g/cm^3) is also plotted for two conditions, when B is set to a value of 1.0, and when B is derived using Eq. (11). When a value of 1.0 is used for B, the calcium content is defined as a proportion of the wet bone weight [18]. When B is applied using Eq. (11), the calcium content is defined as a proportion of the dry bone weight (as required by Eq. (12) and originally defined

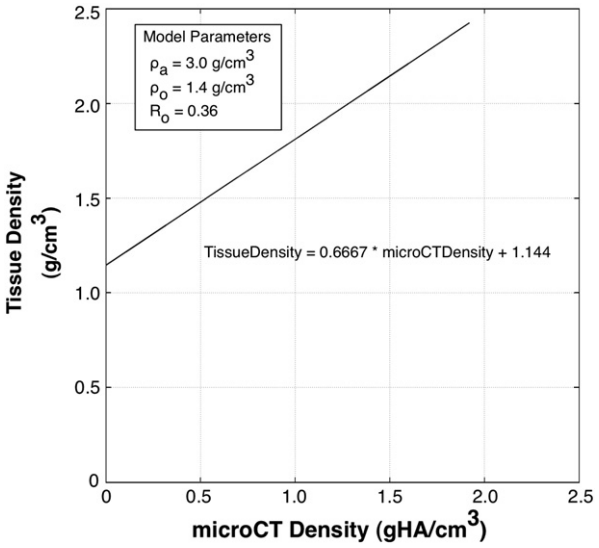

Fig. 1. MicroCT (mineral) density versus tissue density, defined by Eq. (9), for ash constituent density = 3.0 g/cm^3, organics constituent density = 1.4 g/cm^3, and an organics constituent volume fraction of 0.36.

by Currey [36]). This analysis is included because the value of B has been neglected (i.e., implicitly defining $B = 1.0$) in previous implementations of this method and the corresponding effects have not been quantified. For the nominal range of microCT density values (0.4–1.2 gHA/cm^3), using a constant tissue density of 2.0 g/cm^3 in Eq. (10) results in a lower estimate of elastic modulus when compared to the baseline model. When B is applied using Eq. (11), the maximum underestimation of the baseline model occurs at a microCT density of 0.85 gHA/cm^3 and results in a difference of 6.5 GPa (13.8 GPa vs. 7.3 GPa). When B is set to a value of 1.0 (as implemented in Renders et al. [18]), the maximum underestimation of the baseline model occurs at a microCT density of 1.02 gHA/cm^3 and results in a difference of 12.0 GPa (17.9 GPa vs. 5.9 GPa).

Effects of model parameter perturbations on the mineral density versus tissue density and elastic modulus relationships

The effects of perturbing the baseline model parameters based on the ranges defined in the previous section, *Defining average and bounds to the baseline model parameters,* are presented. The effects on the linear relationship relating mineral and tissue density (Eq. (9)) from the selected model parameter deviations previously described are

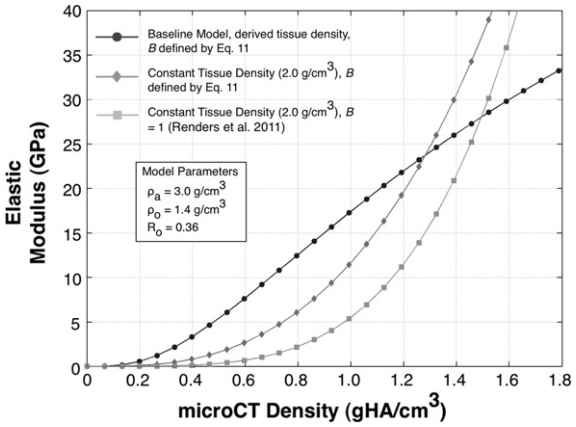

Fig. 2. MicroCT (mineral) density versus elastic modulus. Three relationships are plotted: 1) derived tissue density (baseline model using Eq. (14)), 2) constant tissue density with B defined by Eq. (11), and 3) constant tissue density with B set to a value of 1.0.

Table 2
Effects of baseline model parameter perturbations on the derived relationship between mineral density, tissue density (Eq. (9)), and elastic modulus (Eq. (13)).

Ash density, ρ_a (g/cm^3)	Organics volume fraction (R_o)	Organics density, ρ_o (g/cm^3)	Tissue v. mineral density equation constants (Eq. (9))		Tissue density (g/cm^3)		Elastic modulus (GPa)	
			Slope (m)	Intercept (b)	@ 0.4 gHA/cm^3	@ 1.2 gHA/cm^3	@ 0.4 gHA/cm^3	@ 1.2 gHA/cm^3
2.85	0.30	1.10	0.649	1.030	1.29	1.81	7.9	34.0
2.85	0.40	1.10	0.649	1.040	1.30	1.82	4.5	25.6
2.85	0.30	1.45	0.649	1.135	1.39	1.91	4.6	26.0
2.85	0.40	1.45	0.649	1.180	1.44	1.96	2.4	18.4
3.20	0.30	1.10	0.688	1.030	1.31	1.86	7.9	34.0
3.20	0.40	1.10	0.688	1.040	1.32	1.87	4.5	25.6
3.20	0.30	1.45	0.688	1.135	1.41	1.96	4.6	26.0
3.20	0.40	1.45	0.688	1.180	1.46	2.01	2.4	18.4
3.0[a]	0.36	1.40	0.667	1.144	1.41	1.94	3.3	22.0

[a] The values in this row correspond to the baseline model (Fig. 1).

summarized in Table 2. The effect of the model parameter perturbations on the tissue density and elastic modulus for two values of microCT Density (0.4 and 1.2 gHA/cm^3) is also included in Table 2. As previously described, ash density is the only parameter that affects the slope of the tissue versus mineral density equation. A 10.9% decrease in ash density resulted in a corresponding 5.6% decrease in the slope of the linear equation relating mineral and tissue density. For $R_o = 0.3$, $\rho_o = 1.10$ g/cm^3, and a tissue mineral density of 1.2 gHA/cm^3, a decrease in ash density from 3.2 to 2.85 g/cm^3 resulted in a decrease in calculated tissue density from 1.855 to 1.809 g/cm^3, or 2.5%.

The perturbation of the model parameters presented in Table 2 demonstrates that the elastic modulus was influenced by the density and volume fraction of the organics constituent. The organics constituent density (ρ_o) inversely influenced the predicted elastic modulus with the maximum elastic modulus decrease of 42% (7.9 to 4.6 GPa) being observed for a 32% increase in organics density (1.1 to 1.45) for the low TMD value of 0.4 gHA/cm^3. The corresponding elastic modulus decrease at 1.2 gHA/cm^3 decreased by 24% (34.0 to 26.0 GPa). A similar inverse relationship was observed for the organics volume fraction (R_o) with an elastic modulus decrease of 43% (7.9 to 4.5 GPa) resulting from a 33% increase in organics volume fraction (0.3 to 0.4). Interestingly, ash density does not have an effect on the predicted elastic modulus. This is also supported by direct examination of Eq. (13), which does not include the ash density (ρ_a) parameter. This is a direct result of the constituent approach used here and how Eq. (12) was originally defined by Currey [36], which was to use as input the calcium content per g-dry defatted bone. Presented another way, the numerator of [Ca] is the calcium content (mgCa) of a bone voxel, which is dependent on the tissue mineral density (ρ_{HA}) and voxel volume in the derivation presented and not the ash density. The denominator, or the equivalent weight of dry defatted bone for that same voxel volume, can be defined as the calcium content (i.e., mineral weight) plus the weight of the organics constituent (water has been removed). Combining those two values results in the theoretical derivation of [Ca], which is observed in Eq. (13) as $\rho_{HA}/(\rho_{HA} + \rho_o \cdot R_o)$.

Discussion

A theoretical relationship relating microCT mineral density to tissue density and elastic modulus was defined. The derivation utilizes prior knowledge of the bone constituents' volume fractions and individual constituent densities to calculate the volume and mass of each constituent within a microCT scanned bone voxel. Perturbations to the assumed constituent densities were applied to evaluate the sensitivity on the derived tissue density and subsequently calculated elastic modulus.

The theoretical tissue versus mineral density relationship depicted in Fig. 1 is similar to a previously reported relationship derived using a combination of empirical and constitutive assumptions. Raum et al. [31], using tissue mineral density (TMD) values measured with synchrotron microCT data from the diaphysis of 10 human radii, derived an empirical relationship between the ratio of organics to water volume fraction as a function of the volume fraction of the mineral to develop the following polynomial relationship relating TMD and tissue density:

$$\rho_t = 1.12\left(\mathrm{g/cm^3}\right) + 0.73 \cdot \mathrm{TMD} - 0.033\left(\mathrm{cm^3/g}\right) \cdot \mathrm{TMD}^2.$$

Similar to our derivation, Raum et al. [31] utilized the contributions of individual bone constituents (assuming ash and organic densities of $\rho_a = 3.0$ g/cm^3 and $\rho_o = 1.41$ g/cm^3, respectively) and assumed that TMD (ρ_{HA}) is an equivalent measure of the ash content per voxel volume. The polynomial equation fits the previously collected data with an $R^2 = 0.999$ and RMSE = 0.009. The intercept of the polynomial equation (1.12 g/cm^3) is very similar to the theoretically derived intercept presented here of 1.144 g/cm^3 for the baseline model and falls within the range of intercepts presented in Table 2. For TMD values of 0.4 and 1.2 gHA/cm^3, the polynomial derived by Raum et al. [31] yields tissue densities of 1.41 and 1.94 g/cm^3, which match the theoretically derived values of the baseline model (Table 2). Although the polynomial equation is non-linear by definition, the response is nearly linear over the range plotted in Fig. 1 (0 to 1.92 gHA/cm^3) and very closely matches the theoretical derivation with baseline model parameters of Eq. (9). The maximum absolute difference between Eq. (9) (with the baseline model parameters) and the polynomial equation (over the 0 to 1.92 gHA/cm^3 mineral density range) occurred at a tissue mineral density of 1.92 gHA/cm^3 with a difference of 0.034 g/cm^3, or 1.4% of the predicted tissue density of 2.42 g/cm^3 using Eq. (9).

The relationship between elastic modulus and microCT density presented in Eq. (14) is similar to previously published results from several nanoindentation experiments. Turner et al. [42] determined the elastic modulus for dehydrated cortical and cancellous bone using nanoindentation applied to two specimens taken from the femur of a single human donor. The average elastic modulus for trabecular and cortical bone was 18.14 and 20.02 GPa, respectively. From Eq. (14), those average elastic moduli correspond to microCT densities of 1.03 and 1.11 gHA/cm^3, which are in the nominal range of bone and close to the value of 1.2 gHA/cm^3 many use as the microCT density for fully mineralized bone. Mulder et al. [11] performed a combined nanoindentation and microCT experiment and correlated the tissue stiffness (GPa) and tissue mineral density (gHA/cm^3) for corresponding locations of trabecular bone sites from dehydrated mandibular condyles of four newborn pig specimens. Mulder et al. [11] presented the linear equation based on the sampled data relating the two variables for the approximate range of 0.4 to 0.8 gHA/cm^3 of:

$$\text{Elastic Modulus (GPa)} = 25 \cdot \mathrm{TMD}\left(\mathrm{gHA/cm^3}\right) - 5.83.$$

For the same range of 0.4 to 0.8 gHA/cm^3, the baseline model (Eq. (14)) predicts elastic moduli of 3.34 and 12.55 GPa, which are similar to those predicted by Mulder et al. [11] of 4.17 and 14.17 GPa, respectively. In a separate experiment with a similar protocol and

specimens, Mulder et al. [6] fit a polynomial relationship from data with an approximate range of 0.6 to 0.9 gHA/cm^3. The baseline equation presented here predicts the elastic modulus for the tissue mineral densities of 0.6 and 0.9 gHA/cm^3 as 7.68 and 15 GPa, and similar to the linear equation [11], the polynomial equation [6] slightly overestimates the values predicted here with values of 9.28 and 16.7 GPa, respectively.

Two assumptions were made in the derivation of the theoretical relationship between tissue and tissue mineral density. The first assumption was that the underlying constituents of bone are composed of water, organics, and ash and that those constituent densities are defined as 1.0, 1.4 g/cm^3, and 3.0 g/cm^3, respectively. It is accepted that bone can be modeled as a composition of water, organics, and ash [43], however the constituent densities of those components are not universally accepted, which prompted the evaluation of the derived relationship for different constituent densities. Ash constituent density (ρ_a) was shown to only affect the slope of the theoretical relationship between tissue mineral and tissue density. This is conceptually consistent with the physical makeup of bone. For example, if ash density affected the intercept of the tissue mineral versus tissue density relationship, this would imply that the density of osteoid (when no ash is present) is affected by the density of a material (ash) that is not present, which is not consistent. A change in ash density from 3.2 to 2.85 g/cm^3 (10.9% difference) was evaluated for a constant tissue mineral density of 1.2 gHA/cm^3 and resulted in approximately a 2.7% change in calculated tissue density. The sensitivity of tissue density to the range of tested ash densities was small for commonly observed bone tissue mineral densities. The effect of the organics constituent density on tissue density is confounded by the assumed volume fraction of the organics constituent and is discussed in conjunction with that assumption.

The second assumption was that the volume fraction (R_o) of the organic constituent of bone is constant, which implies that any changes in the ash constituent volume are directly proportional to equivalent changes in the water constituent volume [35]. Robinson [32] raised this same question when he asked "…as to what moieties of the matrix constituents did leave the matrix during the mineralization process." Robinson [32] goes on to describe the biological process of mineralization and states that "in all the bone observed from regions where bone was being deposited the matrix appeared before the apatite crystals and the collagen fibrils at least were not apparently replaced or displaced by the apatite crystals." Collagen is the primary component of the organics constituent (89% as defined in Martin et al. [43]), which bounds the potential error of the stated assumption to potentially 11% of the remaining organics constituent as possibly being displaced. Deakins [33] similarly observed that the mineral being deposited in the incisor enamel matrix of certain rodents displaced an equivalent water volume and that most of the organic matrix was left behind. Parfitt [44] stated "mineralization increases the density of the newly formed bone but does not alter the volume, since water is displaced by solid mineral". The assumption that the volume fraction of the organics constituent is constant (and that mineral displaces only water) is therefore consistent with the literature.

The value of the organics constituent volume fraction (R_o) and density (ρ_o) affects the intercept of the linear relationship between tissue and tissue mineral density. The values of reported organics constituent density in the literature range from 1.1 to 1.45 g/cm^3, with the majority of reported values being close to 1.4 g/cm^3. A value of 1.4 g/cm^3 was selected for the baseline model to use consistent density and organic constituent volume fraction measures from one source [28]. The variations in volume fraction (0.3–0.4) and density (1.1–1.45 g/cm^3) of the organics constituent, evaluated together, resulted in a change of 0.15 g/cm^3 in the intercept location relating tissue and tissue mineral density. For the worst-case situation in which the organic constituent variation would have the most effect (i.e., when tissue mineral density = 0 gHA/cm^3), the corresponding change in tissue density was approximately 15%. The percent difference decreases as tissue mineral density increases and at a tissue mineral density of 1.2 gHA/cm^3, the difference in computed tissue density decreases to approximately 8%. If all the parameter variations (ρ_a, ρ_o, and R_o) are taken together, the span of calculated tissue densities for the tissue mineral density values of 0.4 and 1.2 gHA/cm^3 are 0.165 and 0.196 g/cm^3, respectively, or approximately 13% and 11% of the minimum tissue densities calculated for those tissue mineral density values.

One limitation to the method described above is related to the assumption that a complete bone voxel is used as input (i.e., partial volume effects and/or substantial voids, e.g., Haversian canals, have been removed). Therefore, pre-processing of the scanned image to segment out the bone material appropriately is required. The application of this method without proper segmentation could result in the misidentification of non-bone material as bone tissue. For example, if the method described previously were applied to a voxel of non-bone material (i.e., fat or marrow) with a microCT density value of 0 gHA/cm^3, that voxel of material would be misinterpreted as bone with no mineral (i.e., osteoid) and assigned a tissue density (1.144 g/cm^3 for the baseline model described by Fig. 1) based on the assumed density of the organics and water constituents and the assumed organics constituent volume fraction. The constituent based derivation also assumes that any non-bone material in the bone voxel is appropriately modeled as having a density equivalent to water and that the contribution of those entities to the volume of a given bone voxel is negligible.

Another limitation of the derivation is related to the inherent assumption that the equivalent density measured from the microCT scanner can be directly used to calculate ash content. Raum et al. [31] utilized a similar assumption when developing a polynomial relationship between microCT measured density and tissue density. However, Nazarian et al. [45] measured tissue mineral density (defined as equivalent density) using a microCT scanner for 21 bovine cortical specimens and compared that to measured ash density and found an average difference of 0.185 g/cm^3. The difference was partially attributed to the type of calibration phantom (liquid versus solid) used to calibrate the microCT scanner, however, that a measurable difference existed raises several questions related to the proposed derivation. First, the mineral content computed using the microCT mineral density (and voxel volume) for each voxel may not be equivalent to the ash content of bone contained within that voxel. Schileo et al. [46] found that the ash and CT derived densities of grouped trabecular and cortical bone specimens were highly correlated ($R^2 = 0.997$), but that the fit line (intercept: −0.09, slope: 1.14) was statistically different than the quadrant bisector. Ash and microCT mineral density were shown to be equivalent at 0.643 g/cm^3. For a microCT mineral density of 1.2 gHA/cm^3, the equivalent ash density was 1.13 g/cm^3. Schileo et al. [46] recommended a correction be applied to the CT derived bone mineral density to yield an accurate estimate of ash density that did not underestimate for low-density tissue nor overestimate for high-density tissue values. Such a correction factor is potentially machine and calibration phantom dependent and was not applied in the presented derivation but could easily be implemented by applying the proposed correction factor in Eq. (4). Second, the microCT scan parameters, beam-hardening correction, and calibration phantom may influence the ratio of mineral content (microCT) versus true ash content. The second issue may be compounded with the recent finding that there exists a non-linear relationship between linear attenuation and hydroxyapatite (HA) density [47]. This effect has largely been ignored in the literature due to the limited availability of microCT calibration phantoms with a maximum HA density over 0.8 gHA/cm^3, even though normal bone can have HA density values over 50% higher than that maximum.

The effect of ignoring the wet/dry weight correction factor (B) and utilizing a constant tissue density for deriving the calcium content weight fraction had significant effects on the calculated elastic modulus when compared with the baseline model. For a representative TMD value of 1.0 gHA/cm^3, the baseline model resulted in a calculated elastic modulus of 17.4 GPa. Assuming a constant tissue density of 2.0 g/cm^3 resulted in a calculated modulus decrease to

11.6 GPa. When the calcium content weight fraction was not applied (i.e., Ca/g-wet defatted bone was used instead of Ca/g-dry defatted bone) the calculated modulus decreased further to 5.5 GPa. Due to the non-linear difference between the three stiffness versus microCT density relationships (Fig. 2), the stress/strain gradients, in addition to the overall magnitudes, produced from a microFE model with applied stiffness heterogeneity from the different cases would result in substantially different results. Validation of the proposed relationships to experimental testing remains necessary, yet the potential 68% decrease in assigned elastic modulus for a single TMD value illustrates the importance of the assumptions applied and that assigning tissue stiffness heterogeneity derived from microCT TMD data is not trivial.

The efficacy of utilizing the equation developed by Currey [36] for defining microCT scale voxel based material properties must be evaluated in further detail. The equation was developed using data from 23 different species and included tissue (i.e., elephant tusk) not traditionally classified as 'bone.' Currey [36] clearly showed that the calcium content in bone is proportional to measured elastic modulus. However, Currey [36] also stated that the data showed a large range of elastic moduli, "particularly in the region between 230 and 280 mg calcium g^{-1} bone," which includes a large range of the data presented. One limitation of this implementation is that the anisotropic nature of bone is ignored. The influence of the collagen content and structure is also ignored even though they have been suggested to affect fracture strength and the ability of the bone to absorb energy [48]. Additionally, the mechanical bending test used to determine the elastic modulus was performed on bone specimens with a size of $30 \times 2 \times 3.5$ mm, substantially larger than the microCT voxel size (10 to 80 μm) to which the moduli are being assigned here. As bone is inherently hierarchical in structure, the elastic modulus should vary as the length scale changes, however, the magnitude of this effect is not known. The implementation of Currey's equation proposed here assumes that the porosity of the thresholded bone in each microCT voxel is negligible. For a subset of the data in which porosity was calculated, Currey showed that incorporating porosity in the regression (in addition to calcium content alone) improved the prediction of elastic modulus. This suggests that a subset of samples (i.e., the specimens with low porosity) may be more appropriate in developing an equation for use with microCT data. In spite of these limitations, the combined implementation (Eq. (14)) that incorporates Currey's equation matches well with previous experiments [6,11,42].

This study presents a method for estimating voxel-based tissue density and isotropic elastic modulus from microCT derived tissue mineral density (gHA/cm^3). The approach relies on three parameters well studied in the literature, the density of the ash constituent in bone, the density of the organics constituent in bone, and the volume fraction of the organics constituent. In addition to providing a means for quantifying the tissue density of bone on a voxel by voxel basis from microCT scan data, this approach defines a more accurate application of previously published methods used to assign heterogeneous material properties (elastic modulus) to micro finite element models.

Role of funding source

Dept of Veterans Affairs, Rehab R&D Service (Proj. A6816R).

Acknowledgments

This study was supported by the Dept of Veterans Affairs, Rehab R&D Service (Proj. A6816R). Authors' roles: Study design: DW, DL, and GB. Data collection: DW. Data analysis: DW. Data interpretation: DW and GB. Drafting manuscript: DW and GB. Revising manuscript content: DW, DL, and GB. Approving final version of manuscript: DW, DL, and GB. DW takes responsibility for the integrity of the data analysis.

References

[1] Boutroy S, Bouxsein ML, Munoz F, Delmas PD. In vivo assessment of trabecular bone microarchitecture by high-resolution peripheral quantitative computed tomography. J Clin Endocrinol Metab 2005;90:6508–15.
[2] Dalzell N, Kaptoge S, Morris N, Berthier A, Koller B, Braak L, et al. Bone micro-architecture and determinants of strength in the radius and tibia: age-related changes in a population-based study of normal adults measured with high-resolution pQCT. Osteoporos Int 2009;20:1683–94.
[3] Kazakia GJ, Hyun B, Burghardt AJ, Krug R, Newitt DC, de Papp AE, et al. In vivo determination of bone structure in postmenopausal women: a comparison of HR-pQCT and high-field MR imaging. J Bone Miner Res 2008;23:463–74.
[4] Khosla S, Riggs BL, Atkinson EJ, Oberg AL, McDaniel LJ, Holets M, et al. Effects of sex and age on bone microstructure at the ultradistal radius: a population-based noninvasive in vivo assessment. J Bone Miner Res 2006;21:124–31.
[5] Borah B, Ritman EL, Dufresne TE, Jorgensen SM, Liu S, Sacha J, et al. The effect of risedronate on bone mineralization as measured by micro-computed tomography with synchrotron radiation: correlation to histomorphometric indices of turnover. Bone 2005;37:1–9.
[6] Mulder L, Koolstra JH, den Toonder JMJ, van Eijden TMGJ. Relationship between tissue stiffness and degree of mineralization of developing trabecular bone. J Biomed Mater Res A 2008;84:508–15.
[7] van Ruijven LJ, Mulder L, van Eijden TMGJ. Variations in mineralization affect the stress and strain distributions in cortical and trabecular bone. J Biomech 2007;40:1211–8.
[8] Burghardt AJ, Kazakia GJ, Ramachandran S, Link TM, Majumdar S. Age- and gender-related differences in the geometric properties and biomechanical significance of intracortical porosity in the distal radius and tibia. J Bone Miner Res 2010;25:983–93.
[9] Miller LM, Little W, Schirmer A, Sheik F, Busa B, Judex S. Accretion of bone quantity and quality in the developing mouse skeleton. J Bone Miner Res 2007;22:1037–45.
[10] Morgan EF, Mason ZD, Chien KB, Pfeiffer AJ, Barnes GL, Einhorn TA, et al. Micro-computed tomography assessment of fracture healing: relationships among callus structure, composition, and mechanical function. Bone 2009;44:335–44.
[11] Mulder L, Koolstra JH, den Toonder JMJ, van Eijden TMGJ. Intratrabecular distribution of tissue stiffness and mineralization in developing trabecular bone. Bone 2007;41:256–65.
[12] Zioupos P, Cook RB, Hutchinson JR. Some basic relationships between density values in cancellous and cortical bone. J Biomech 2008;41:1961–8.
[13] Pistoia W, van Rietbergen B, Lochmüller E-M, Lill CA, Eckstein F, Rüegsegger P. Image-based micro-finite-element modeling for improved distal radius strength diagnosis: moving from bench to bedside. J Clin Densitom 2004;7:153–60.
[14] Verhulp E, van Rietbergen B, Müller R, Huiskes R. Indirect determination of trabecular bone effective tissue failure properties using micro-finite element simulations. J Biomech 2008;41:1479–85.
[15] Newitt DC, Majumdar S, van Rietbergen B, von Ingersleben G, Harris ST, Genant HK, et al. In vivo assessment of architecture and micro-finite element analysis derived indices of mechanical properties of trabecular bone in the radius. Osteoporos Int 2002;13:6–17.
[16] Bourne BC, van der Meulen MCH. Finite element models predict cancellous apparent modulus when tissue modulus is scaled from specimen CT-attenuation. J Biomech 2004;37:613–21.
[17] Mulder L, van Ruijven LJ, Koolstra JH, van Eijden TMGJ. Biomechanical consequences of developmental changes in trabecular architecture and mineralization of the pig mandibular condyle. J Biomech 2007;40:1575–82.
[18] Renders GAP, Mulder L, van Ruijven LJ, Langenbach GEJ, van Eijden TMGJ. Mineral heterogeneity affects predictions of intratrabecular stress and strain. J Biomech 2011;44:402–7.
[19] Cioffi I, van Ruijven LJ, Renders GAP, Farella M, Michelotti A, van Eijden TMGJ. Regional variations in mineralization and strain distributions in the cortex of the human mandibular condyle. Bone 2007;41:1051–8.
[20] Renders GAP, Mulder L, van Ruijven LJ, van Eijden TMGJ. Degree and distribution of mineralization in the human mandibular condyle. Calcif Tissue Int 2006;79:190–6.
[21] Renders GAP, Mulder L, Langenbach GEJ, van Ruijven LJ, van Eijden TMGJ. Biomechanical effect of mineral heterogeneity in trabecular bone. J Biomech 2008;41:2793–8.
[22] Day JS, Bone Quality: The Mechanical Effects of Microarchitecture and Matrix Properties [dissertation], Rotterdam, Netherlands, Department of Orthopaedics, Erasmus Medical Center (2005) 195 pp.
[23] Hernandez CJ, Beaupré GS, Keller TS, Carter DR. The influence of bone volume fraction and ash fraction on bone strength and modulus. Bone 2001;29:74–8.
[24] Boivin G, Meunier PJ. The degree of mineralization of bone tissue measured by computerized quantitative contact microradiography. Calcif Tissue Int 2002;70:503–11.
[25] Wagner DW, Beaupre GS. Letter to the Editor referring to the article "Mineral heterogeneity affects predictions of intratrabecular stress and strain" published in Journal of Biomechanics (volume 44, Issue 3, Pages 402–407). J Biomech 2011;44:1826–7.
[26] Bouxsein ML, Boyd SK, Christiansen BA, Guldberg RE, Jepsen KJ, Müller R. Guidelines for assessment of bone microstructure in rodents using micro-computed tomography. J Bone Miner Res 2010;25:1468–86.
[27] Burghardt AJ, Kazakia GJ, Laib A, Majumdar S. Quantitative assessment of bone tissue mineralization with polychromatic micro-computed tomography. Calcif Tissue Int 2008;83:129–38.
[28] Martin RB. Porosity and specific surface of bone. Crit Rev Biomed Eng 1984;10:179–222.

[29] Fajardo RJ, Cory E, Patel ND, Nazarian A, Laib A, Manoharan RK, et al. Specimen size and porosity can introduce error into uCT-based tissue mineral density measurements. Bone 2009;44:176–84.
[30] Sips RJA, Mulder L, Koolstra JH, van Eijden TMGJ. Development of the micro architecture and mineralization of the basilar part of the pig occipital bone. Connect Tissue Res 2008;49:22–9.
[31] Raum K, Cleveland RO, Peyrin F, Laugier P. Derivation of elastic stiffness from site-matched mineral density and acoustic impedance maps. Phys Med Biol 2006;51:747–58.
[32] Robinson RA. Physicochemical structure of bone. Clin Orthop Relat Res 1975;112:263–315.
[33] Deakins M. Changes in the ash, water, and organic content of pig enamel during calcification. J Dent Res 1942;21:429–35.
[34] Roschger P, Fratzl P, Eschberger J, Klaushofer K. Validation of quantitative backscattered electron imaging for the measurement of mineral density distribution in human bone biopsies. Bone 1998;23:319–26.
[35] O'Flaherty EJ. Physiologically based models for bone-seeking elements. I. Rat skeletal and bone growth. Toxicol Appl Pharmacol 1991;111:299–312.
[36] Currey JD. What determines the bending strength of compact bone? J Exp Biol 1999;202:2495–503.
[37] Elliott SR, Robinson RA. The water content of bone. I. The mass of water, inorganic crystals, organic matrix, and CO_2 space components in a unit volume of the dog bone. J Bone Joint Surg Am 1957;39-A:167–88.
[38] Gong JK, Arnold JS, Cohn SH. Composition of trabecular and cortical bone. Anat Rec 1964;149:325–31.
[39] Currey JD. Physical characteristics affecting the tensile failure properties of compact bone. J Biomech 1990;23:837–44.
[40] Gong JK, Arnold JS, Cohn SH. The density of organic and volatile and non-volatile inorganic components of bone. Anat Rec 1964;149:319–24.
[41] Bear RS. The structure of collagen molecules and fibrils. J Biophys Biochem Cytol 1956;2:363–8.
[42] Turner CH, Rho J, Takano Y, Tsui TY, Pharr GM. The elastic properties of trabecular and cortical bone tissues are similar: results from two microscopic measurement techniques. J Biomech 1999;32:437–41.
[43] Martin RB, Burr DB, Sharkey NA. Skeletal tissue mechanics. New York, USA: Springer Verlag; 1998.
[44] Parfitt AM. The physiologic and clinical significance of bone histomorphometric data. In: Recker R, editor. Bone histomorphometry. Techniques and interpretations. Boca Raton, FL, USA: CRC Press; 1983. p. 143–223.
[45] Nazarian A, Snyder BD, Zurakowski D, Muller R. Quantitative micro-computed tomography: a non-invasive method to assess equivalent bone mineral density. Bone 2008;43:302–11.
[46] Schileo E, Dall'ara E, Taddei F, Malandrino A, Schotkamp T, Baleani M, et al. An accurate estimation of bone density improves the accuracy of subject-specific finite element models. J Biomech 2008;41:2483–91.
[47] Deuerling JM, Rudy DJ, Niebur GL, Roeder RK. Improved accuracy of cortical bone mineralization measured by polychromatic microcomputed tomography using a novel high mineral density composite calibration phantom. Med Phys 2010;37:5138–45.
[48] Marcus R. Osteoporosis, vol. 1. Elsevier Academic Press; 2008.